

# NEW JOURNAL OF CHEMISTRY

## SUPPLEMENTARY MATERIAL

### **Nano- and microstructured silver films synthesised by halide-assisted electroless plating**

F. Muench,<sup>\*a</sup> B. Juretzka,<sup>a</sup> S. Narayan,<sup>a,b</sup> A. Radetinac,<sup>a</sup> S. Flege,<sup>a</sup> S. Schaefer,<sup>a</sup> R. W. Stark<sup>a,b</sup> and W. Ensinger<sup>a</sup>

<sup>a</sup> Department of Materials and Geoscience, Technische Universität Darmstadt, Alarich-Weiss-Straße 2, 64287, Darmstadt, Germany.

<sup>b</sup> Center of Smart Interfaces, Technische Universität Darmstadt, Alarich-Weiss-Straße 10, 64287, Darmstadt, Germany.

\* corresponding author: muench@ca.tu-darmstadt.de

#### **S1: Comparison of the 3D structure of pristine and Ag-coated polycarbonate foil**

Using confocal laser scanning microscopy, the topographies of pristine polycarbonate foil and polycarbonate foil coated with the compact Ag film version were compared. The Ag film was deposited using the halide-free plating bath and a reaction time of 24 h. As can be seen in Fig. S1, the structure of the polymer is still clearly visible after Ag deposition, which however adds some fine-grained texture to the material. As calculated from the 3D maps (Fig. S1 e,f), the  $S_q$  values (polymer: 1.0  $\mu\text{m}$ ; Ag-coated polymer: 1.0  $\mu\text{m}$ ) and the  $S_z$  values (polymer: 7.7  $\mu\text{m}$ ; Ag-coated polymer: 7.3  $\mu\text{m}$ ) of both surface types are very similar. These observations are in correspondence with the SEM investigations (see e.g. Fig. 1 a,b).

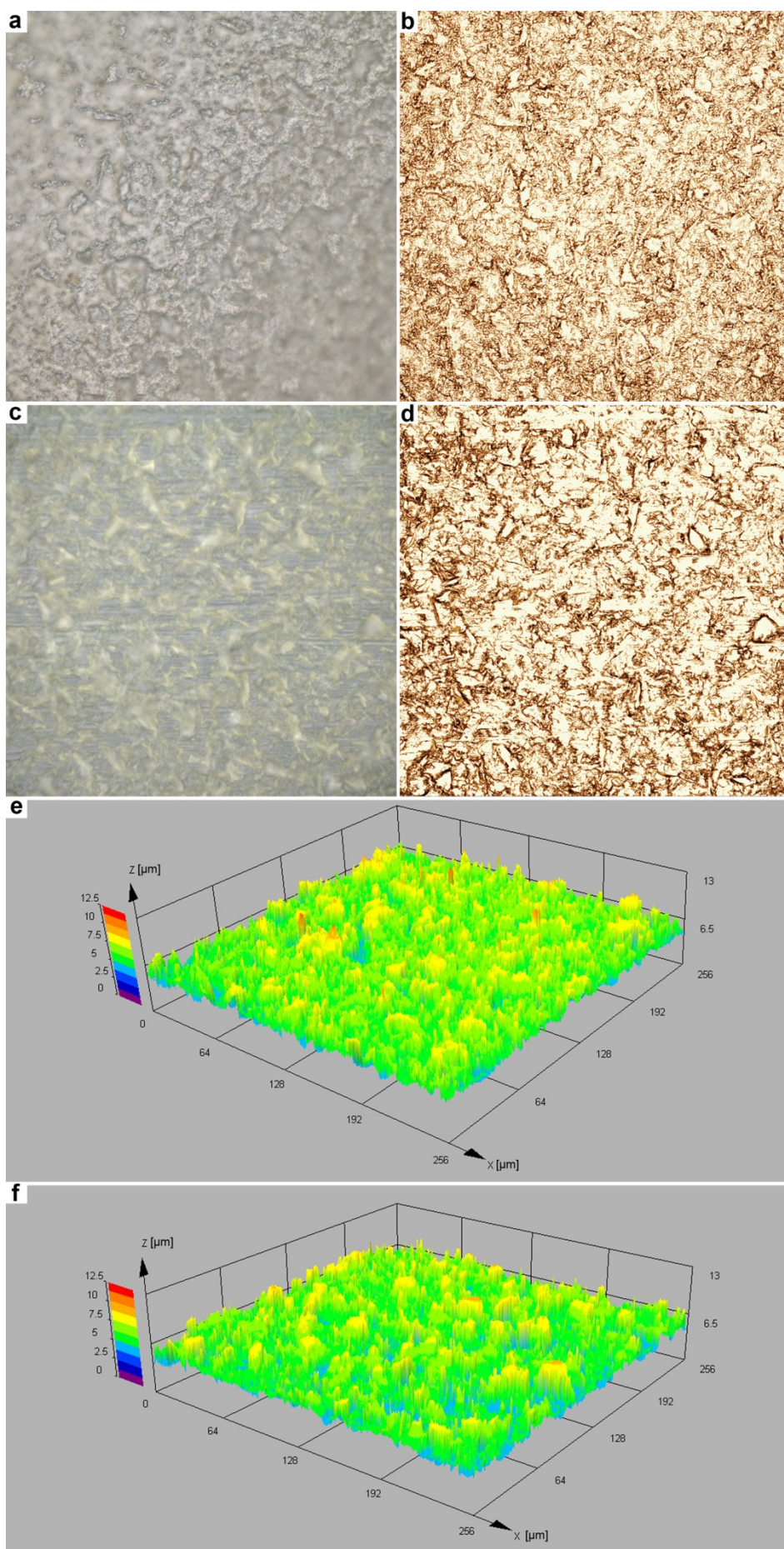


**Fig. S1.** Microscopy images of a,b) Ag-coated polycarbonate foil and c,d) pristine polycarbonate foil, recorded at 50-fold magnification (left column: conventional microscopy, right column: confocal laser scanning microscopy). 3D maps of e) the Ag-coated polycarbonate foil and f) the pristine polycarbonate foil.

## **S2: 3D structure of the microparticle-island containing Ag film before and after Au exchange**

Using confocal laser scanning microscopy, the effect of the Au exchange step on the roughness parameters was evaluated. The Ag film obtained from a bath containing 1 mM  $\text{Cl}^-$  (7 d deposition time) was subjected to galvanic replacement, and the topographies of both the original and the modified films were measured (Fig. S2). While both films clearly show a different color (Fig. S2 a,c), their calculated roughness parameters are very similar ( $S_q$  values: Ag film: 1.2  $\mu\text{m}$ ; Au-exchanged film: 1.2  $\mu\text{m}$ ;  $S_z$  values: Ag film: 7.8  $\mu\text{m}$ ; Au-exchanged film 8.5  $\mu\text{m}$ ). This observation is related to the limitation of the structural changes to a length scale (see Fig. 6 c,d) which is below the resolution limit of this technique. Thus, AFM was used to analyze this reaction step (see section S3).

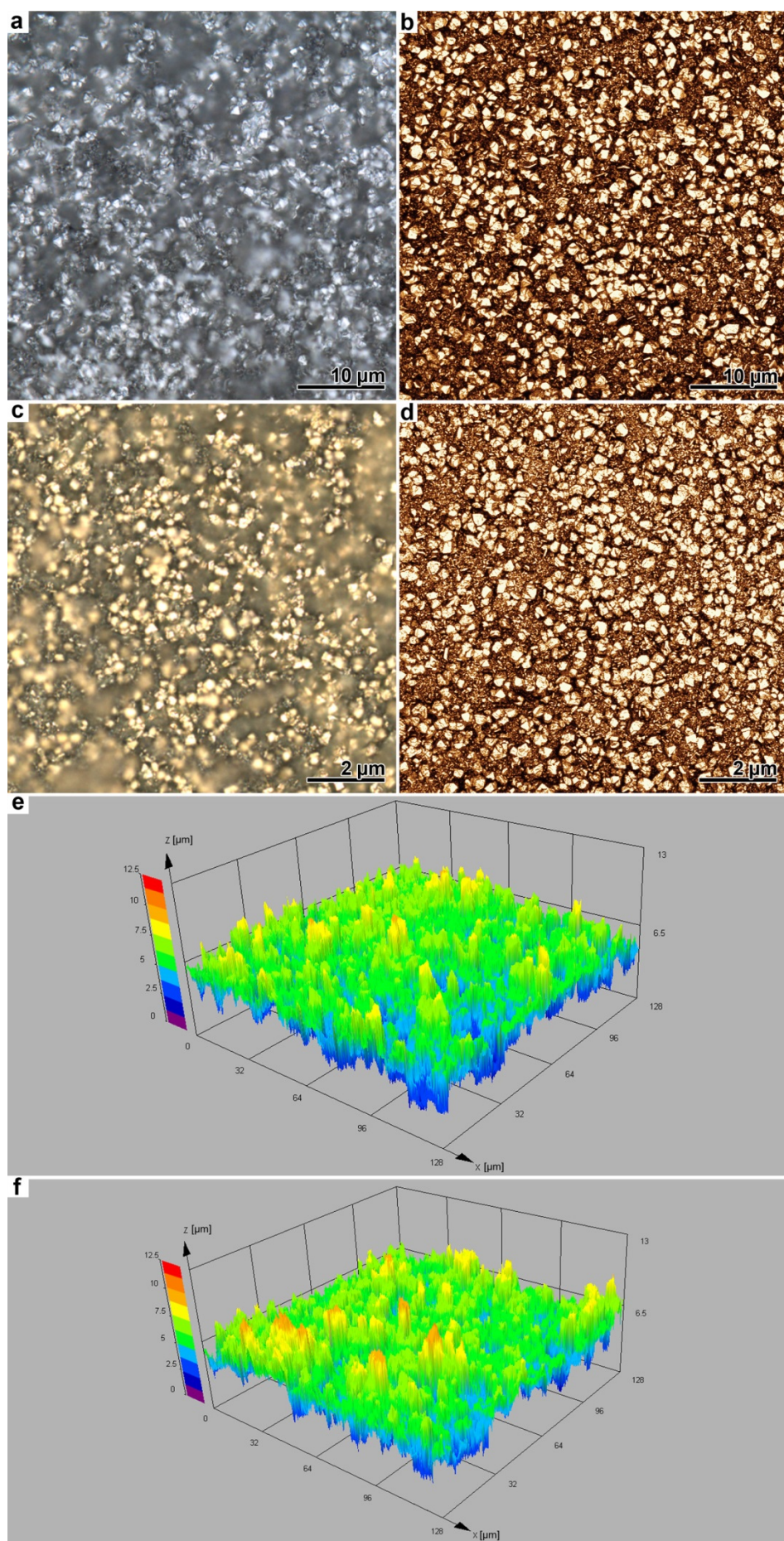


**Fig. S2.** Microscopy images of Ag coatings obtained using 1 mM  $\text{Cl}^-$  a,b) before and c,d) after galvanic replacement with Au, recorded at 100-fold magnification (left column: conventional microscopy, right column: confocal laser scanning microscopy). 3D maps of e) the Ag film and f) the Au-etched Ag film.

### S3: AFM investigation of the structural changes during Au exchange

In the case of all surface types used for the hydrophobicity measurements (see Fig. S1 and Fig. S2), height differences of multiple micrometers are found, which prohibited analysis by atomic force microscopy. To gain more insights about the structural changes induced by the galvanic replacement reaction, a new set of samples was prepared. Smooth polymer foils were coated with the standard Ag film (no halide addition, 24 h deposition time). Thus, large microscale features stemming either from the substrate roughness or the deposition of isolated, enlarged Ag particles were avoided, and the overall sample was suitable for AFM analysis. Optionally, the as-obtained Ag-coated polymer was subjected to Au exchange. The results of the AFM measurements are shown in Fig. S3. The typical surface features observed in the SEM studies (Fig. 1 a,b; Fig. 6 c,d) can also be found in the AFM images. The pure Ag film can be described as a dense aggregate of particles with a comparatively smooth nanoscale surface structure (Fig. S3 a,b), while the Au-etched metal film develops a cauliflower-like surface structure with roundish features in the size range of few tens of nm, which is interrupted by cavities of several 100 nm size (Fig. S3 c,d). Thus, galvanic replacement increases the roughness of the metal film in the nanoscale and submicron regime (Ag film: root mean square roughness = 60 nm; Au-exchanged film: root mean square roughness = 150 nm).

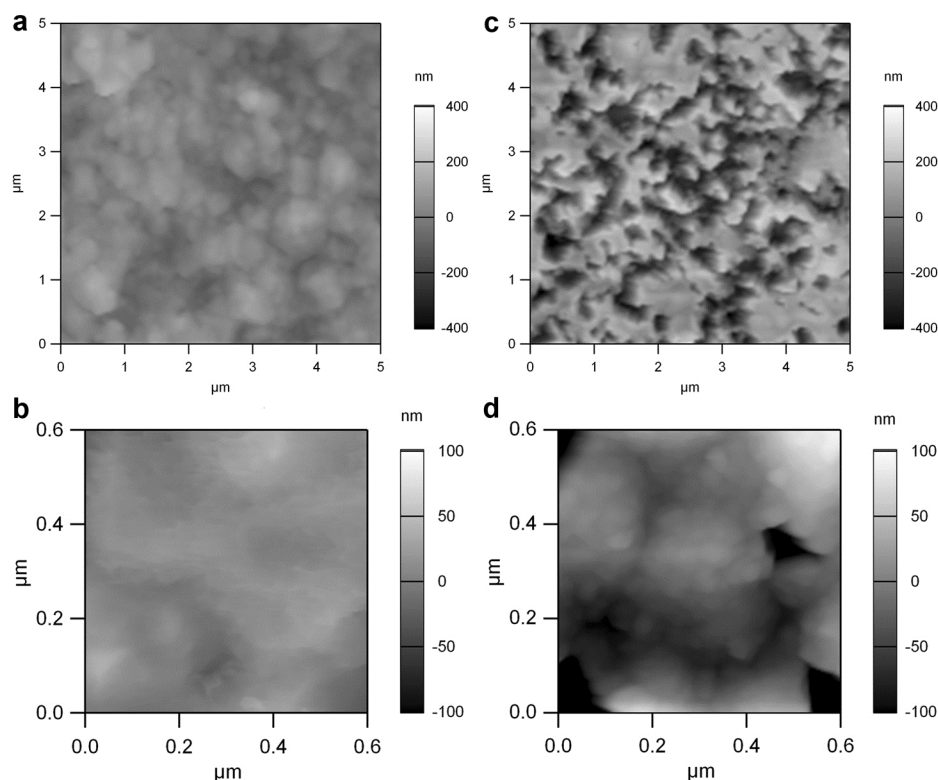


**Fig. S3.** AFM images of different coatings on smooth polymer surfaces. a,b) Ag film obtained after 24 h deposition in a halide-free plating bath. c,d) Otherwise identical Ag film which had been exchanged with Au.

#### **S4: Contact angle hysteresis during tilt**

Water drops were placed on the different surfaces, followed by tilting. The contact angle hysteresis was determined just before the drops started to slide. Representative photographs for all four surface types can be found in Fig. S4. Compared to the precursor materials A and B, the additional nanostructuring of the samples A2 and B2 resulted in significantly reduced roll off angles and hysteresis values. Sample B2 with its hierarchical structure excels in the self-cleaning properties, as can be seen by its extremely low hysteresis and tilt angle.

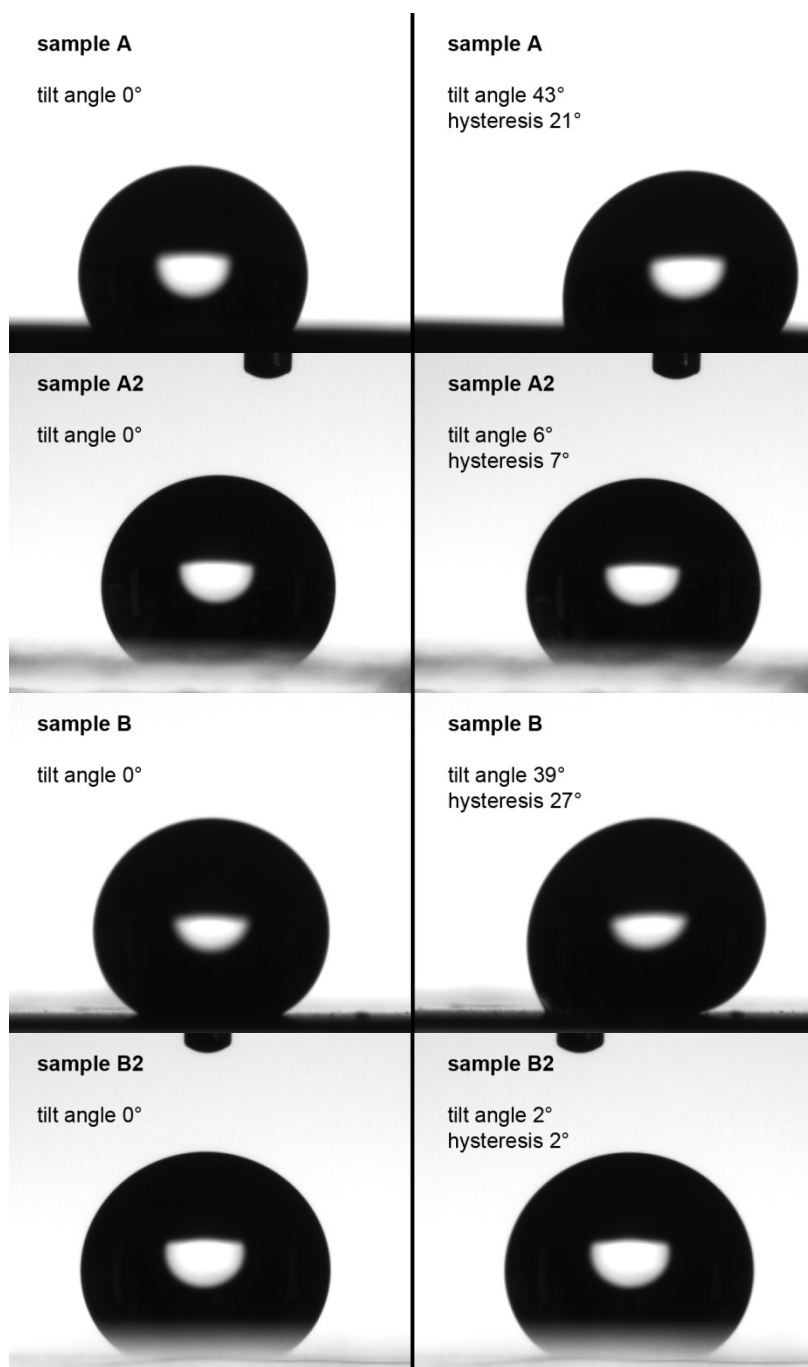


**Fig. S4.** Photographs of water drops on the different surface types. The left column shows the drops directly after placement, the right column shows them at tilt angles just before their roll off.

### S5: Contact angle hysteresis during tilt

Without the thiol self-assembly step, lower contact angles were found for all coating types (Fig. S5). In the case of the pure Ag coatings, distinctly decreased contact angle values were obtained (sample A:  $86 \pm 3^\circ$ ; sample B:  $58 \pm 3^\circ$ ). The contact angle of hydrophilic surfaces usually decreases with increasing roughness [Y. Li, G. Duan, G. Liu, W. Cai, Chem. Soc. Rev. 42 (2013) 3614]. Accordingly, the reduced contact angle in the case of surface B can be explained by the additional structuring due to the halide addition. In the case of the Au-exchanged surfaces, relatively high contact angles were found (sample A2:  $149 \pm 8^\circ$ ; sample B2:  $140 \pm 6^\circ$ ). This can be explained by the simultaneous change of the roughness and the surface energy during galvanic replacement reaction (e.g. by adsorption of the hydrophobic quarternary ammonium salt, which is a component of the exchange solution; see. e.g. [J. P. Vivek, I. J. Burgess, Langmuir 28 (2012) 5031]). Although the Au-exchanged samples remained close to the superhydrophobicity criterion (contact angle =  $150^\circ$ ), none of the surfaces could be considered self-cleaning. The water droplets could be easily placed, and pronounced pinning was observed. In all cases, drops stuck to the surface even at a tilt angle of  $90^\circ$ .

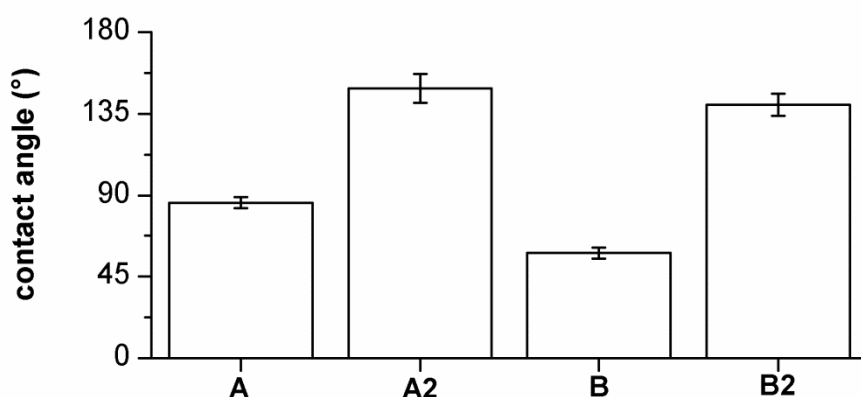


**Fig. S5.** Static contact angles of the four thiol-free surface types (water droplets, 8  $\mu$ L volume).

## S6: Proof of principle for the fabrication of flexible, conductive materials

A rectangular polymer strip ( $2 \times 4$  cm) was electrolessly coated with Ag (Fig. S6 a). Using four point probe measurements, the resistivity of the metal thin film was determined as  $1.26 \cdot 10^{-4} \Omega \text{ cm}$ , which is in the range of values reported for electrolessly plated Ag [A. Inberg, Y. Shacham-Diamand, E. Rabinovich, G. Golan, N. Croitoru, Thin Solid Films 389 (2001) 213]. During repeated bending (angle alternating between 0 and  $180^\circ$ ), the resistivity of the film did not change significantly (Fig. S6 b).

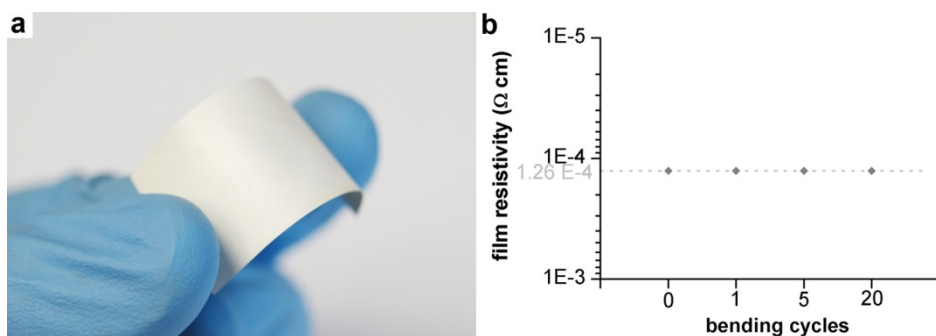


**Fig. S6.** a) Photograph of the metallized polymer strip. The Ag deposition was performed without halide addition for 24 h. b) Resistivity of the Ag film in dependence of the number of times the strip was bent.